Corma Canós, A.; Martínez, C.; Doskocil, E. (2013). Designing MFI-based catalysts with improved catalyst life for C-3(=) and C-5(=) oligomerization to high-quality liquid fuels. Journal of Catalysis. 300:183-196. doi:10.1016/j.jcat.2012.12.029

# Designing MFI based catalysts with improved catalyst life for $C_3^=$ and $C_5^=$ oligomerization to high quality liquid fuels.

Avelino Corma[a]*, Cristina Martínez[a], Eric Doskocil[b]

[a] Instituto de Tecnología Química (UPV-CSIC), Universidad Politécnica de Valencia- Consejo Superior de Investigaciones Científicas, Avenida de los Naranjos s/n, 46022 Valencia, Spain.

[b] BP Products North America Inc., 150 West Warrenville Rd., Naperville, IL 60563, USA.

* Corresponding author: acorma@itq.upv.es ; Tel: (34) 963877800, FAX: (34) 963879444

**Abstract.**

Light olefin oligomerization is an important alternative for the production of clean liquid automotive fuels, and can be performed in the presence of solid acid catalysts. Among them, medium pore zeolites, and especially ZSM-5, have been widely described in the open literature. In this work the relative importance of intracrystalline diffusion path lengths for the product molecules (depending on the zeolite crystal size and presence of mesopores in the crystallites) and Brønsted acid site density are discussed for two different olefins, propene and 1-pentene. Thus, ZSM-5 samples with a) the same crystallite size and different acid site density, b) the same density of acid sites and different crystallite size, c) post-synthesis generation of mesopores by different desilication severity, and d) samples with similar crystal size, mesoporosity and acid site density, but with a different ratio of external to internal acid sites, have been prepared and studied for oligomerization of propene and 1-pentene. The results obtained suggest that the properties required for a best performing catalyst (maximum conversion and lowest deactivation rate) are different for these two alkenes. Whereas

Brønsted acid site density is determinant for propene oligomerization when intracrystalline diffusion path lengths are below a certain critical value, the presence of a high number of Brønsted acid sites is not sufficient in the case of 1-pentene, and additional mesoporosity becomes crucial. Thus, mesoporous ZSM-5 samples prepared by post-synthesis desilication treatments present a larger improvement in initial conversion and catalyst life for 1-pentene oligomerization than for conversion of propene.

**Keywords:**

Oligomerization, liquid fuels, ZSM-5 zeolites, desilication, hierarchical zeolites, mesoporous zeolites, diesel, Brønsted acid site density, catalyst deactivation.

## 1. Introduction

Oligomerization of light alkenes, such as propene and butenes, represents an important route to the production of environmentally friendly synthetic liquid fuels, free of sulfur and aromatics [1-6]. The process allows production of olefinic mixtures in the range of gasoline and diesel. Thus, depending on the operating conditions and catalyst used, the ratio of diesel to gasoline can be modified [2-4]. In fact, high temperatures (>300ºC) and low pressures (≤30 bar) increase gasoline yield, whereas lower temperatures and higher pressures will favor the formation of heavier oligomers within the diesel fraction. Concerning the catalysts, different solid acids have been described for the oligomerization of olefins in the open [2-3, 7-20] and in the patent literature [1, 21-32]. Among them, medium pore zeolites with either mono- or tridirectional pore systems have been the most successful, mainly for vapor phase oligomerization processes [2-3, 20-21]. Other structures, such as the monodirectional 10-R ZSM-22 [33], ZSM-57 [34], with 10R- channels provided with wide lobes, or large pore ZSM-12 [35] and USY [36] zeolites have also been described for oligomerization of C3=-C6= in supercritical or liquid phase, and are commercially applied [6]. If one considers a carbocation mechanism for olefin oligomerization, it is clear that in the absence of geometrical constraint, highly branched - high molecular weight products would be formed. Thus, from the point of view of the fuel product quality (especially diesel) and catalyst life, it is desirable to obtain less branched molecules while avoiding the formation of heavier products, which will remain adsorbed within the catalyst pores leading to a relatively fast deactivation, at least when the reaction is carried out in the gas phase. Therefore, in this specific case, medium pore zeolites (and especially ZSM-5) have been the preferred catalysts for C3= and C4= oligomerization to produce gasoline and diesel, while larger pore zeolites are rapidly deactivated [13-14, 17]. Nevertheless, for oligomerization reactions that produce larger molecules with higher boiling points and higher heats of adsorption than the reactants, it will be mandatory to design a medium pore zeolite catalyst with optimum acid site density and textural properties. These

parameters should be even more critical when larger olefins (C5=) have to be oligomerized [12, 16, 18].

In this work, we have studied how the different catalyst parameters influence activity, selectivity and catalyst life, and the optimization of a ZSM-5 based catalyst for oligomerization of propene and 1-pentene on the bases of its physicochemical properties. Then, ZSM-5 samples with a) the same crystallite size and different acid site density, b) the same density of acid sites and different crystallite size, c) post-synthesis generation of mesopores by different desilication severity, and d) samples with similar crystal size, mesoporosity and acid site density but with a different ratio of external to internal acid sites, have been prepared and studied for oligomerization of propene and 1-pentene. The role played by the different catalyst parameters on their catalytic behavior will be shown, as well as the fact that the key variable determining activity and selectivity for ZSM-5 is different when the objective is C3= oligomerization or when the olefin to be oligomerized is C5=.

## 2. Experimental

### *2.1 Catalyst preparation*

The starting ZSM-5 samples were supplied by Zeolyst (CBV3020, CBV5020, CBV8020) and TRICAT (TZP322, TZP302A and TZP302H) in their ammonium form. Desilication treatment was performed by contacting the as supplied zeolites with a basic solution of NaOH heated at the desired treatment temperature, under vigorous stirring. The liquid to solid ratio used was 33 in weight. After the desired time, the solid was separated by filtration and washed with deionized water until lowering the pH to a value of 7.0. The Na-zeolite was then washed with a 0.8 M oxalic acid solution for 2 h, at 70ºC, for selective dealumination of the external surface. The dealuminated zeolite was separated from the solution by filtration, washed and finally calcined at 375ºC for 3hours. The samples were named as *M-MFI-T-t-OX*, where *M* is the NaOH solution

concentration, *MFI* is the parent ZSM-5 zeolite, e.g. TZP322 or CBV5020, *T* is the treatment temperature, *t* the duration of the desilication, and *–OX* states for the oxalic acid treatment. Exceptionally the Na-zeolite obtained after the basic desilication was ion exchanged with a 2.5 M $NH_4Cl$ solution (L/S=10, T=80ºC, t=1 hour, refluxed under vigorous stirring), washed with deionized water until chloride free, and dried overnight at 100ºC. This ion exchange treatment was repeated twice before calcination in a muffle for 3 hours at 500ºC. The ammonium exchanged samples were labeled as *M-MFI-T-t-A*. For comparison purposes, sample TZP322 was calcined (HTZP322) and then, in the acid form, it was treated with a 0.5 M alkaline solution for 90 min at 85ºC, and finally selectively dealuminated by means of an oxalic acid treatment, as described above. This sample was named as 0.5-HTZP322-85-90-OX.

### *2.2 Catalyst characterization*

The chemical composition of the catalysts was determined in a Varian-715-ES Inductivity-Coupled Plasma Analyzer (ICP). X-ray diffraction (XRD) was used to assess the purity and relative crystallinity of the different MFI zeolite samples. XRD patterns were obtained at room temperature in a Philips X'pert diffractometer using monochromatized CuK$\alpha$ radiation. Textural properties were obtained from nitrogen adsorption isotherms, measured at 77 K (-196ºC) using an ASAP 2000 Micromeritics instrument. The micropore volume of the products was calculated by the t-plot method, and the mesopore volume according to the BJH correlation. The acidity of the zeolites was determined by infrared spectroscopy combined with adsorption-desorption of pyridine at different temperatures. Infrared spectra were measured with a Nicolet 710 FT IR spectrometer. Pyridine adsorption–desorption experiments were carried out on self-supported wafers (10 mg·cm$^{-2}$) of original samples previously activated at 400ºC and $10^{-2}$ Pa for 2 h. After wafer activation, the base spectrum was recorded and pyridine vapor ($6.5\times10^{2}$ Pa) was admitted into the vacuum IR cell and adsorbed onto the zeolite. Desorption of pyridine was performed in vacuum over three consecutive 1 h periods of heating at 150, 250, and 350ºC, each followed by an IR measurement at room temperature. All

the spectra were scaled according to the sample weight. The amount of Brønsted and Lewis acid sites was determined from the intensities of the bands at ca. 1545 and 1450 $cm^{-1}$, respectively, using the molar extinction coefficients given by Emeis [37].

Scanning electron microscopy (SEM) was performed using a Jeol JSM 6399 microscope (20 KV) equipped with a secondary electron images detector using gold-coated powder specimens.

Transmission Electron Microscopy (TEM) characterization was carried out in a Philips CM10 (100 kV) microscope. Before TEM observation, the samples were prepared by suspending the solid in isopropanol, ultrasonicating for 1 min and placing one drop on a carbon coated copper grid (300 mesh).

Solid State $^{27}Al$ MAS NMR spectra were recorded in a Varian Unity VXR-400WB spectrometer, at 104.2 MHz with a spinning rate of 7 kHz and a 9º pulse length of 0.5 µs with a 0.5 s repetition time. Chemical shifts were reported relative to $[Al^{3+}(H_2O)_6]$.

X-ray photoemission spectra (XPS) were recorded in a SPECS spectrometer equipped with a Phoibos 150 9MCD detector using a non-monochromatic Al X-ray source operating at 200 W. The samples were pressed into a small disc and evacuated in the pre-chamber of the spectrometer at $1 \cdot 10^{-9}$ mbar. Quantitative data were calculated from the Al2p and Si2p peak intensities after nonlinear Shirley-type background subtraction and corrected by the transmission function of the spectrometer. The CasaXPS software was used for spectra processing.

*Catalytic tests*

The catalytic experiments were performed in a 10 mm internal diameter down-flow stainless steel fixed bed reactor, at 200ºC, 4.0 MPa, and contact time ranging from 0.08 to 0.17 h. In these conditions the reaction occurs in the gas phase. The catalyst (0.25 mm and 0.42 mm particle size) was diluted in all cases with SiC (0.64 mm-0.25 mm) to obtain a bed volume of 4.0 $cm^3$. In these conditions a plug flow pattern was ensured [38]. The temperature in the catalyst

bed was controlled by means of two independent heating zones with the corresponding thermocouples properly placed inside the catalytic bed. Before reaction, the catalysts were activated in-situ by increasing temperature up to 520ºC in $N_2$ flow (200 ml/min) at a rate of 2.0 º/min and calcination in air flow (200 ml/min) at 520ºC for 5 h. Then the reactor was cooled down to the reaction temperature in a flow of $N_2$ (200 ml/min). The olefinic mixture was fed to the reactor as a liquid by means of a Gilson piston pump, and the pressure was controlled during the reaction electronically through a Badger pneumatic valve.

For the propene oligomerization experiments, the olefin was co-fed (in the liquid phase) with propane in a 60:40 propene:propane molar mixture. This mixture simulates a typical refinery feedstock containing light alkenes, where alkanes are always present [26]. The liquid C5+ products were condensed in a cold trap at the exit of the reactor, whereas the non-condensable vapors entered an on-line chromatograph. The on-line analysis of the unconverted reactants and of the lightest reaction products (not condensed in the cold trap) were performed at periodic intervals in a Varian 3400 chromatograph equipped with a 30m Plot/$Al_2O_3$ column and a FID detector. The liquids collected in the trap were analyzed by simulated distillation (SIMDIS) in a Varian 3800 equipped with a 10 m, 0.53 mm ID MXT-2887 metal column supplied by Restek Corp., and the software STAR SD from Varian following the ASTM D-2887 standard.

For discussion, the selectivity results are referred to by the naphtha, diesel and heavy product fractions, determined by SIMDIS according to the following cut points:

| | |
|---|---|
| Naphtha: | C5-173.9ºC |
| Diesel: | 173.9-391.1ºC |
| Heavy fraction: | 391.1-1000ºC |

Experiments were performed to confirm the absence of interphase (external) and intraphase (internal) gradients [38] under the whole range of experimental conditions used here.

As in the case of propylene oligomerization, for the 1-pentene conversion tests, the olefin was co-fed with n-heptane, in a 60:40 1-pentene:heptane molar mixture. The full reactor outlet stream was vaporized and analyzed with an on-line Varian 3400 gas-chromatograph. The unconverted reactants and products were separated in a 60 m, 0.25 x 0.25 TRB-5 column and quantified by means of a FID detector. n-Heptane was used as internal standard. Moreover, the C5+ mixture was condensed for further analysis by simulated distillation, in the same conditions and using the same temperature cuts as for the C3=:C3 feed, but excluding n-heptane from the naphtha fraction.

## 3. Results and discussion

### 3.1 Catalyst preparation and characterization.

#### *3.1.1 ZSM-5 samples non modified by post-synthesis treatments.*

The physico-chemical properties of the commercial, as supplied, ZSM-5 samples, are enclosed in table 1. These samples can be divided into two groups. Zeolyst zeolites (CBV-) present similar and relatively small crystal size (below 0.6 μm) and differ mainly in their Si/Al ratio. As a first estimation, and based on the SEM and TEM pictures enclosed in figures 1 and 2, respectively, the size of the individual crystallites of the Zeolyst zeolites is difficult to deduce, but aggregates are clearly visible, especially for CBV3020, and the differences in crystal size are not negligible, with samples CBV3020 and -5020 presenting smaller individual crystallite sizes than sample CBV8020. The three TRICAT samples (TZP-) have a similar Si/Al ratio (Si/Al ~10) and cover a wide range of crystal sizes, going from the nano-crystalline TZP322 (20-50 nm) to the micron-sized TZP302H (see figures 1 and 2). In order to have a more accurate crystal size

distribution a particle count has been performed on the SEM images and the histograms obtained are shown in Figure SI1 (in the supplementary information). Moreover, the average crystal size obtained from the values measured is given in table 1.

All samples present textural properties typical of an MFI structure, with BET surface areas close to 400 $m^2/g$ and micropore volumes around 0.150 $cm^3/g$. The larger BJH mesopore volume obtained for CBV3020, CBV5020 and TZP322 is due to their small crystal size and the corresponding intercrystalline porosity.

The similar chemical composition of the TRICAT samples is in good agreement with their close Brønsted acidity values obtained by FT-IR spectroscopy combined with pyridine adsorption and desorption at increasing temperatures (table 2). It is important to note that all the acid hydroxyls are accessible to pyridine (see figure SI2 in the supplementary information), even for sample TZP302-H, with the largest crystals. The Zeolyst samples, with Si/Al molar ratios varying in a range from 15 to 40, present lower total Brønsted acidity than the TRICAT samples, in agreement with their lower Al content. However, additional factors may contribute to this lower acidity. In fact, the larger amount of Lewis acid sites measured on CBV3020, as compared to any of the TRICAT samples, indicates that this sample has a larger proportion of aluminum in extra-framework positions (EFAL). Part of this EFAL may be neutralizing bridging hydroxyl groups, decreasing in this way the acidity even further. The higher dealumination of sample CBV3020 is also evidenced by the $^{27}Al$ MAS NMR results shown in figure 3. There it can be seen that the TRICAT samples only present the band at 59 ppm corresponding to tetrahedrally coordinated aluminum (figure 3-b), whereas CBV3020 (and also CBV8020, although less pronounced) presents an additional band at 0 ppm assigned to octahedral EFAL (figure 3-a). It is important to remark here that all the samples have been characterized as supplied (in their ammonic form) without any modification (except for the “in-situ” thermal treatment under vacuum previous to the IR measurements). In order to confirm that this *in-*

*situ* treatment of the samples does not modify the acidity, samples CBV3020 and CBV5020 were calcined ex-situ in a down-flow fixed bed reactor following the activation protocol described in the experimental section, their acidity was measured by FT-IR combined with pyridine adsorption, and the acidity loss as compared to the samples only pretreated under vacuum for the IR experiments was below 10% (data not shown).

*3.1.2 Post-synthesis modified ZSM-5 samples.*

Controlled desilication by mild basic treatments has proved to be an efficient method for generating secondary mesoporosity in MFI type zeolites, among others [39-42]. This additional pore system facilitates the access of bulky reactants to the active sites, but also enhances the diffusion of bulky products out of the zeolite structure before fouling of the micropore structure occurs. Depending on the characteristics of the starting zeolite (Si/Al ratio and crystal size), the basic treatment may also deaglomerate the individual crystallites when dealing with nano-sized materials and, in some cases, reduce the crystal size [43]. According to a recent study [44] these treatments do not modify the properties of the remaining micropore system, or the intrinsic strength of the active Brønsted acid sites. Although none of these active sites have been detected in the mesopores, a direct consequence of the additional mesoporosity is the reduction of the intracrystalline diffusion paths and, therefore, the fraction of Brønsted acid sites located near the pore entrance is higher as compared to non-modified zeolites. Thus, considering the results obtained in the former section, one may predict that this type of mesoporous zeolites obtained by post-synthesis treatments can be of interest in oligomerization of light olefins. Indeed, the extension of catalyst deactivation due to the formation of heavy oligomers is expected to be reduced in these samples, similarly to what has been described for other reactions involving bulky reactants or products [39]. Thus, two of the commercial ZSM-5 samples, TZP322 and CBV5020, (the best performing when tested as supplied, as will be shown in the next section) have been treated with NaOH aqueous solutions

of different concentrations and at different times and temperatures, with the aim of modifying the textural properties of the parent zeolites. The physico-chemical properties and the yields of zeolite produced are presented in table 3. All samples have been treated with oxalic acid after the desilication step, except one of the preparations, 0.5-TZP322-85-90-A, which has been activated by conventional ammonium exchange for comparison purposes.

According to the results enclosed in table 3, low NaOH concentrations (0.2M) do not desilicate zeolite TZP322 and do not generate additional mesoporosity, in agreement with previous results [40]. Base solutions of 0.5M or higher and significantly longer treatment times (90 min) are necessary for modifying the textural properties of this Al-rich ZSM-5. It is important to note that even the most severe desilication treatments do not significantly modify the micropore volume of the final samples, whereas the mesopore volume increases up to values of 0.5 $cm^3/g$ when desilicating TZP322 (see table 3). This is due to the combination of the basic desilication coupled with the oxalic acid selective dealumination step. In fact, the characterization results enclosed in table 3 show that the oxalic acid washing after the NaOH treatment increases the bulk Si/Al ratio, not only by acid dealumination of the external surface, as can be deduced from the XPS values of some selected samples shown in the same table, but also by washing out EFAL species. Moreover, when comparing the oxalic acid treated zeolite with the sample activated by exchanging with $NH_4^+$ followed by a final calcination, we can see that the final micro- and mesopore volumes are significantly higher for the oxalic acid treated catalyst (see table 3). The lower EFAL content of sample 0.5-TZP322-85-90-OX has also been confirmed by $^{27}Al$ MAS NMR measurements (see figure 3-c), and is also reflected in a lower amount of Lewis acid sites as measured by pyridine adsorption (see table 4). Verboekend et al. [40] have recently described that it is possible to recover a fraction of the crystallinity and micropore volume of desilicated ZSM-5 zeolites, ion-exchanged and calcined after the basic leaching in order to obtain the acid form, by post-treating the samples with mild acid –HCl- solutions. According to our results it is possible to obtain ZSM-5 with high mesopore

volumes and with micropore volume reductions lower than 10% in a single step by treating the desilicated zeolite directly with oxalic acid. Moreover, the oxalic acid treatment is highly effective in selectively decreasing the amount of Al located near the external surface of the crystals, as shown by the XPS results enclosed in Table 3. In fact, an increase is observed in the Si/Al ratio determined by XPS when comparing the parent TZP322 with the oxalic acid treated, TZP322-OX, or when comparing the two desilicated samples, 0.5-TZP322-85-90-A and 0.5-TZP322-85-90-OX. The selective dealumination step with oxalic acid increases significantly the external Si/Al ratio as compared to the bulk composition given by ICP, and this is expected to improve the quality of the diesel obtained by reducing the branching degree of the final products [21, 45].

Concerning the Brønsted acidity of these TZP322 based samples, table 4 shows that it is reduced in all cases as compared to the parent zeolite, even for sample 0.2-TZP322-85-30-OX, subjected to a milder NaOH treatment that did not increase its mesopore volume. In order to evaluate if this acidity loss is a consequence of the oxalic treatment, the starting zeolite TZP322 has been selectively dealuminated with oxalic acid (sample TZP322-OX) under the same conditions as the desilicated samples were treated. The overall Si/Al ratio is decreased to 14 and the mesopore volume is considerably increased just by washing with oxalic acid (table 4). However, due to the low amount of EFAL of the parent TZP322 (see figure 3-a), framework dealumination takes place in a large extent, and the Brønsted acidity of the selectively dealuminated ZSM-5, TZP322-OX, is considerably reduced as compared to the parent zeolite (see table 4). This will result in a worse catalytic behavior of TZP322-OX as compared to the non-modified ZSM-5 for oligomerization of $C_3^=$, as will be shown later.

Regarding zeolite CBV5020, generation of mesoporosity by desilication treatments is easier on this sample due to its lower Al content [40]. The final oxalic acid treatment reduces the Al content of the desilicated samples even more, and this results in a reduction of their total

Brønsted acidity, given in table 4. As could be expected because of the lower acidity of the parent CBV5020, when compared to TZP322, the Brønsted acidities of the modified CBV5020 samples are also significantly lower, in all cases, than those of the basic treated TZP322.

Figure 4 shows representative TEM images of the desilicated TZP322 and CBV5020 samples, compared at the same magnifications. The pictures evidence the formation of mesoporosity, as well as the larger extension of the base attack produced on the CBV5020, as compared to TZP322, when treated with the lowest 0.2 M NaOH concentration.

## 3.2 Catalytic tests.

### *3.2.1. Propene oligomerization.*

In the first place commercial ZSM-5 zeolites with different Al content (different density of active sites) and different crystallite size (different diffusion path lengths within the crystals) have been studied without further modification, except for an *in-situ,* down flow calcination as described in the experimental section. The main purpose of this preliminary study is to determine the influence of those chemical and morphological properties on the catalytic behavior of the MFI catalysts for propene oligomerization to higher chain olefins in the range of fuels.

The catalytic activity obtained with non-modified TRICAT and Zeolyst ZSM-5 zeolites in the oligomerization of propene, under industrially relevant conditions [2], is shown in figure 5. Important differences can be seen in initial activity and in the catalyst deactivation rate among the different catalysts. The highest activity is obtained with sample TZP322, which presents the smallest crystal size but also the highest Brønsted acidity. TZP322 is followed by CBV5020 and CBV3020, which also have very small crystal size (average values below 200 nm), but with about half the number of Brønsted acid sites as compared to the former. Among these two

samples, CBV3020, with larger EFAL content, is less active and deactivates slightly faster than CBV5020. Moreover, as shown in figures 1 and 2, the small crystallites of CBV3020 are grouped in larger crystal aggregates, instead of being well defined, isolated crystals as in the case of CBV5020 or TZP322. TZP302A and TZP302H, despite their highly acidic nature, are the less active samples. These two ZSM-5 samples present the largest crystallites, and the lower initial activity and higher deactivation rate can be ascribed to possible intracrystalline diffusion problems, especially of the bulkier oligomerized products. This assumption is reasonable, and in fact, Peratello et al., in a thorough thermodynamic and kinetic study concluded that propylene oligomerization is limited by mass transfer even within the 20 Å diameter pores of a mesoporous silica-alumina (MSA) [19] when pure MSA granules were used. With a proper conformation of the catalyst pellets, by dispersing the MSA material in an alumina binder, they were able to reduce this limitation. An optimized catalyst conformation is, however, beyond the scope of the present work. Zeolite CBV8020, with an intermediate crystal size but with the lowest Brønsted acidity, presents an intermediate behavior.

If we attempt to correlate the activity of the catalysts with the zeolite properties presented before, it appears that the most important zeolite variable for propene oligomerization is crystal size, in such a way that initial activity and catalyst life of the large crystal size ZSM-5 is low, even for samples with a large number of acid sites. In fact, the large crystals of TZP302A and TZP302H, combined with their high number of active sites, lead to a drastic deactivation of the catalyst due to fast formation of bulky oligomers, which are not able to exit the microporous structure, and do block the zeolite channels. Thus, small crystal size and short intracrystalline diffusion path lengths are determinant for the good performance of a ZSM-5 zeolite in propene oligomerization. On the other hand, when the reactivity of ZSM-5 zeolites with similar small crystal size is compared, the initial activity and stability towards deactivation correlate quite well with the Brønsted acid site density. This is confirmed in figure 6 where the second order [19] reaction rate constant is plotted as a function of the Brønsted acidity. The

small crystal size ZSM-5, CBV3020, CBV5020, CBV8020 and TZP322 follow a linear trend, whereas the activity of the larger crystal size TZP302A and TZP302H clearly fall out of the trend line.

The deactivation by coking of a zeolite based catalyst is known to be greatly dependent on the zeolite's pore structure [46-47], but also on the process conditions. In the case of ZSM-5, with interconnected channels and no cavities, the access to the active sites is reduced at low coke loadings, but will be blocked at higher coke contents due to location of the coke molecules in the channel intersections [46]. Here we have characterized the spent TZP322 and TZP302H catalysts by elemental analysis (EA), TG-DTA and TPO, in order to see the influence of the crystal size (length of the intracrystalline diffusion paths) on the amount and type of coke formed. The results revealed that, despite the larger amount of carbon remaining in the highly active, small crystal size, TZP322 (33 wt% as determined by EA, with a H/C=2.2 mol/mol), less than 10 % of these carbonaceous residues correspond to coke (burning off at temperatures above 400ºC) and the rest corresponds to adsorbed hydrocarbons retained within the micropores (see figure 7), that desorb at temperatures around 250ºC, with no formation of CO or $CO_2$. Moreover, the mass fragmentation detected by analyzing the TPO outlet stream by mass spectroscopy indicates the aliphatic nature of these hydrocarbons, as could be expected at the low reaction temperatures used [47], and in agreement with earlier work [12, 47]. Only traces of alkylaromatics have been detected, which desorb at temperatures around 310ºC. In the case of the TZP302H sample with large crystals the amount of carbon on the deactivated catalyst is considerably lower (15 wt%, with a H/C molar ratio of 2.3), but the proportion of carbon present as coke (combustion temperature > 400ºC) is higher (29%), and the combustion peak is shifted towards higher temperature (550ºC instead of 500ºC obtained for TZP322). The rest of the carbon corresponds to adsorbed hydrocarbons, similar to those obtained for TZP322, although slightly heavier according to the results of the mass spectrometer connected to the TPO system and to their higher desorption temperature. Thus,

large crystals favor the formation of more and also more refractory coke, which can have a determinant impact on the faster catalyst deactivation, as observed for sample TZP302H.

Regarding product selectivity, the predominant fraction obtained in the C5+ liquids under our experimental conditions is, in all cases, the diesel fraction (see figure 5). It is worth mentioning here that no C1-C4 gas products were detected in significant amounts in any of these tests, and that the products obtained were mainly true oligomerization products (dimers, trimers, tetramers and heavier oligomers as shown in figure SI3) [2]. Nevertheless, there are remarkable selectivity differences among the catalysts compared, which could be ascribed to different factors, including the conversion level. In fact, the two most active zeolites, TZP322 and CBV5020, present a higher selectivity to diesel than the less active CBV3020 and -8020. Moreover, the liquids recovered during the last 3 hours on stream show a slightly higher selectivity to diesel for TZP322 than for CBV5020. This higher production of oligomers in the diesel range obtained with the former can be related to its higher number of Brønsted acid sites and its almost negligible deactivation rate. The low conversion levels obtained with samples TZP302A and TZP302H coupled with the small amount of liquids recovered in these two experiments prevent an accurate determination of their product distribution, which is, therefore, not included in the comparative plots.

What we can learn from this first part of the work on non-modified commercial ZSM-5 samples is that, in order to obtain an active, highly selective to diesel and stable catalyst for propene oligomerization, it is necessary to have short intracrystalline diffusion paths to allow the oligomerization products to easily escape from the micropores. This should avoid further growing of the oligomers and blocking of the channels of the zeolite. This parameter will be even more important when larger olefins, such as pentenes, will be oligomerized, as we will see in the second part of this work.

On the other hand, when crystal size, and therefore also intracrystalline diffusion path lengths, are decreased below a certain critical level, the active site density becomes determinant, and the highest propene conversion is obtained with the catalyst containing the highest number of Brønsted acid sites, e.g., TZP322. Concerning selectivity to the desired fraction, the formation of larger oligomers, belonging to the diesel fraction, is favored by a higher acid site density, provided that diffusion out of the micropores is enhanced by short intracrystalline diffusion path lengths (small crystals).

The catalytic behavior of the modified TZP322 and CBV5020 samples is given in figures 8 through 10. The first thing to be noted from figure 8 is that direct dealumination of the parent TZP322 with oxalic acid, TZP322-OX, has a detrimental effect on the activity of the catalyst, as we have predicted before, probably as a consequence of the Brønsted acidity reduction. Following the same trend, the sample desilicated in milder conditions, 0.2-TZP322-85-30-OX, with no additional mesoporosity but with lower acidity than the starting TZP322, is less active than the parent zeolite. If the severity of the basic treatment is increased, an optimum in activity and stability towards deactivation is observed for sample 0.5-TZP322-85-90-OX. Further increase of the NaOH concentration and of the generated mesopore volume (sample 0.8-TZP322-85.90-OX) do not result in additional benefits, but in a catalyst less active than the best performing 0.5-TZP322-85-90-OX. A possible reason for this is the lower Brønsted acid site density obtained for sample 0.8-TZP322-85-90-OX.

Sample 0.5-TZP322-85-90-A, the desilicated TZP322 zeolite converted into its acid form by conventional ion exchange with $NH_4^+$ followed by calcination, is considerably less active, not only as compared to the corresponding desilicated and oxalic acid treated sample, 0.5-TZP322-85-90-OX (and despite its higher Brønsted acidity) but also as compared to the non-modified TZP322. This can be explained by its lower micropore volume and higher Lewis acidity, which

are directly related to the amount of EFAL present in this sample, EFAL that will partially foul the micropores of the modified zeolite.

Concerning the product distribution, the selectivity to diesel range oligomers is slightly lower for all the desilicated and oxalic acid treated TZP322 samples, as compared to the original zeolite, in good agreement with their reduced Brønsted acid site density. Moreover, the treatments causing a reduction of the Brønsted acidity, without generating additional mesoporosity, result in a larger decrease of the diesel fraction (TZP322-OX and 0.2-TZP322-85-30-OX). If the severity of the desilication is pushed too far, as in 0.8-TZP322-85-90-OX, the selectivity to diesel is also decreased as compared to the parent TZP322, a result that can be explained by the acidity loss. It is important to note that, in order to obtain oligomers in the diesel range, at least four oligomerization steps should take place. Thus, acid site density will have a major influence in this process. When we compare the selectivity results obtained with sample 0.5-TZP322-85-90-A, it is possible to see that, despite its higher acid site density as compared to the sample selectivated with oxalic acid, it is considerably less selective to diesel, also when compared to the parent ZSM-5. This can be directly related to the acid site distribution within the crystallites. Indeed, alkaline desilication treatments are known to enrich the zeolite external surface in aluminum [40] and on these external, more accessible acid sites, the desorption of lighter products (dimers, trimers) will be favored, before they get involved in further consecutive oligomerization steps. Table 3 shows that, in fact, sample 0.5-TZP322-85-90-A presents an external Si/Al ratio of 7, as determined by XPS, which is considerably lower than the value corresponding to the sample 0.5-TZP322-85-90-OX, treated with oxalic acid. One of the purposes of dealuminating with oxalic acid is the selective removal of these external acid sites. This reduction of external acidity will have a double benefit, i.e. it will improve the diesel yield and quality, as it will reduce the branching degree of the final product [21, 45], while increasing the size of the chain by performing more oligomerization events before products will diffuse out of the microporous structure.

Thus, it has been shown that it is possible to increase diesel selectivity by fine-tuning the active site density and acid site distribution by means of a second post-synthesis step (oxalic acid treatment) that decreases the concentration of external acid sites. To better study catalyst deactivation, the experiments have been performed at relatively low contact times (0.17 $h^{-1}$), in order to be able to observe appreciable differences among the catalytic behavior of the samples when performing the oligomerization during six hours time on stream. When increasing the contact times to values of 1 hour or higher, which are more representative of industrial operation, catalytic activity and selectivity to larger oligomers will be enhanced [2].

The usual procedure described for NaOH desilication starts from zeolites in their acid form [39, 41]. In fact, when the samples studied are commercially available in their ammonic form, they are usually calcined before performing the basic treatment [39-40]. Depending on the Si/Al content of the sample, this may result in the generation of EFAL species, which will reduce the micropore volume and the acidity of the zeolite. This phenomenon becomes especially significant for zeolites with low Si/Al ratios, as shown in tables 3 and 4 for the calcined TZP322, H-TZP322. Then, to diminish this potentially negative effect, the modified ZSM-5 samples presented in this work have been prepared by desilication of the ammonic zeolites. For comparison purposes, the acid (calcined) ZSM-5, H-TZP322, has been desilicated in the same conditions as sample 0.5-TZP322-85-90-OX. The characterization results, enclosed in tables 3 and 4, show that the final Si/Al ratio of the sample prepared from the acid form, 0.5-HTZP322-85-90-OX, after the oxalic acid treatment, is considerably higher than that of the sample prepared from the ammonic form, and this results in a significant reduction of the Brønsted acidity of the former. Moreover, the total BET surface area is higher than when starting from the as supplied TZP322, due to a larger mesopore volume. When tested for propene oligomerization at 200ºC, 40 bar pressure and a very low contact time of 0.08 h, sample 0.5-HTZP322-85-90-OX is less active and less selective to diesel (see figure 9). Thus, we can conclude that desilicating the ammonium instead of the acid form of ZSM-5, as it is usually

done, results not only in an improved modified ZSM-5 catalyst for propene oligomerization to diesel, but also in a more efficient procedure since an additional calcination step in the overall preparation protocol is avoided.

Concerning desilicated CBV5020, figure 10 shows that none of the basic treatments applied here has been able to improve either the initial activity or the stability towards deactivation of the parent zeolite. Moreover, the selectivity to diesel is considerably decreased by the desilication. Probably in this case the generation of mesoporosity does not compensate for the reduction in the number of Brønsted acid sites, giving no activity improvement or selectivity enhancement to the desired diesel fraction.

Regarding oligomerization of propene with ZSM-5 zeolite, we can conclude that the key parameters to maximize diesel production are Brønsted acid site concentration and distribution within the crystal, as well as an adequate combination of micro and mesoporosity. The last one can be controlled by modifying crystal size, but also by desilication followed by a partial removal of EFAL by means of a selective dealumination treatment. For zeolite TZP322, an optimum in desilication has been found at a NaOH concentration of 0.5M, a temperature of 85ºC, and a treatment time of 90 min, which gives a mesopore volume of 0.299 cm3/g while preserving 94% of the microporosity. In general, Brønsted acid site concentration and distribution can be modified by controlling the Si/Al ratio of the synthesized sample, as well as by post-synthesis treatments. In our case, post-synthesis desilication and selective dealumination have led to zeolite samples with the adequate Si/Al at the external surface and within the micropores. Optimum treatment involves selective dealumination with 0.8 M oxalic acid at 70ºC for 2 hours after the desilication step described above, and a final calcination at 375ºC for 3 hours.

*3.2 2-Pentene Oligomerization.*

Oligomerization of larger olefins, such as pentenes, is a more demanding process than propene oligomerization, due to the potential formation of larger products with larger coking-pore blocking tendency [12, 18]. Before starting the specific study on ZSM-5 samples, the best performing –non modified- TZP322 zeolite for oligomerization of propene has been tested for conversion of 1-pentene to liquid fuels at two different contact times and under the same temperature and pressure conditions as those used for converting propene. The results enclosed in figure 11 show that, although in the earlier stages of the reaction this ZSM-5 is highly active for converting 1-pentene, the deactivation rate is noticeably higher than for propene oligomerization. Moreover, the main products formed in this case are dimers with boiling points below 173.9ºC that correspond to naphtha. From the above results it appears that oligomerization of 1-pentene will require a further catalyst optimization since it seems to be more prone to catalyst deactivation than in the case of propene.

Results in figure 12 clearly show the improvement in initial activity and stability towards deactivation obtained during 1-pentene oligomerization with sample 0.5-TZP322-85-90-OX, obtained by post-synthesis desilication and oxalic acid dealumination treatment of TZP322. This is especially noticeable at the lowest contact time of 0.08 h. In the case of pentene oligomerization, the benefit of desilication followed by oxalic acid treatment is not limited to the catalytic activity, but it is also evident when comparing the selectivity to the diesel fraction, that can reach values close to 50 wt% when working with the modified ZSM-5. At this point it is important to remark that the selectivity is greatly dependent on contact time used. In fact, figure 12 shows how doubling contact time from 0.08 to 0.17 h results in an increase of the diesel selectivity of more than 10 points, even for the non-modified TZP322. Previous results [2] also suggest that the selectivity to diesel will be higher when performing 1-pentene oligomerization at higher contact times, more representative of industrial processes.

The results presented above confirm that, when dealing with larger olefins such as pentenes, the improvement observed in catalytic activity and selectivity for olefin oligomerization to diesel range products is larger than in the case of propene. This is clear when comparing the results obtained for pentene oligomerization with the parent TZP322, more acidic but with lower mesoporosity, and the modified 0.5-TZP322-85-90-OX, with a more open structure and reduced acid site density. Since pentene needs less oligomerization steps (three) to give a diesel range molecule than propene (four steps), the catalyst requirements to obtain a minimum number of consecutive reactions to reach the target is expected to be different for pentene than for propene oligomerization. Thus, it could be expected that the textural properties of the optimum catalyst for pentene conversion will become a determinant factor, being the presence of mesoporosity more important than to have a high number of Brønsted acid sites, which was key to achieve maximum yield of diesel when working with propene, provided that the intracristalline diffusion paths were below a certain critical value.

## 4. Conclusions.

The comparative study of commercially available ZSM-5 zeolites as catalysts for the oligomerization of propene shows the need for a high Brønsted acid site density and small crystallites in order to have high olefin conversions and high stability towards deactivation with time on stream. In this line, ZSM-5 with mesopores obtained by basic desilication treatments present an improved catalytic behavior only if acidity is sufficiently preserved. When the post-synthesis treatment results in a significant acidity loss, the higher accessibility obtained by the generation of additional mesoporosity is not able to compensate the decrease in the number of active sites.

Catalyst requirements are different when the olefin to be processed is 1-pentene. In this case the products formed are larger (for the same number of oligomerization steps), the risk of micropore fouling-blocking is higher, and catalyst deactivation occurs faster. Thus, the

accessibility presented by the desilicated zeolites becomes crucial and the number of Brønsted acid sites has a smaller influence on pentene conversion and catalyst stability towards deactivation. It appears then that the zeolite oligomerization catalyst should be optimized on the bases of the feed to be converted, and that the presence of a secondary mesopore system will be more advantageous when processing larger olefins.

**Acknowledgements.**

The authors thank BP Products North America and Consolider-Ingenio 2010 (MULTICAT project) for their financial support and permission to publish this work. R. Sanchis is acknowledged for technical support.

**References.**


[1] S.A. Tabak, B.S. Wright, H. Owen, US4504693 (1985), to Mobil Oil.
[2] S.A. Tabak, F.J. Krambeck, W.E. Garwood, AIChE Journal, 32 (1986) 1526-1531.
[3] R.J. Quann, L.A. Green, S.A. Tabak, F.J. Krambeck, Ind. Eng. Chem. Res., 27 (1988) 565-570.
[4] S. Rossini, Catalysis Today, 77 (2003) 467-484.
[5] C. Martinez, A. Corma, Coordination Chemistry Reviews, 255 (2011) 1558-1580.
[6] W. Vermeiren, J.-P. Gilson, Top. Catal., 52 (2009) 31.
[7] C.T. O'Connor, M. Kojima, W.K. Schumann, Applied Catalysis, 16 (1985) 193-207.
[8] A.P. Vogel, C.T. O'Connor, M. Kojima, Clay Minerals, 25 (1990) 355-362.
[9] J.C.Q. Fletcher, J.S. Vaughan, C.T. O'Connor, Preprints - American Chemical Society, Division of Petroleum Chemistry, 36 (1991) 605-612.
[10] R. Catani, M. Mandreoli, S. Rossini, A. Vaccari, Catalysis Today, 75 (2002) 125-131.
[11] M. Casagrande, L. Storaro, M. Lenarda, S. Rossini, Catalysis Communications, 6 (2005) 568-572.
[12] R. Van Grieken, J.M. Escola, J. Moreno, R. Rodriguez, Applied Catalysis, A: General, 305 (2006) 176-188.
[13] M.L. Occelli, J.T. Hsu, L.G. Galya, Journal of Molecular Catalysis, 32 (1985) 377-390.
[14] L.G. Galya, M.L. Occelli, J.T. Hsu, D.C. Young, Journal of Molecular Catalysis, 32 (1985) 391-403.
[15] C.T. O'Connor, R.E. Fasol, G.A. Foulds, Fuel Processing Technology, 13 (1986) 41-51.
[16] C.S. Hsia Chen, R.F. Bridger, Journal of Catalysis, 161 (1995) 687-693.
[17] L.M. Tiako Ngandjui, F.C. Thyrion, Industrial & Engineering Chemistry Research, 35 (1996) 1269-1274.
[18] A. de Klerk, Industrial & Engineering Chemistry Research, 44 (2005) 3887-3893.
[19] S. Peratello, M. Molinari, G. Bellussi, C. Perego, Catal. Today, 52 (1999) 271-277.
[20] G. Bellussi, F. Mizia, V. Calemma, P. Pollesel, R. Millini, Microporous and Mesoporous Materials, 164 (2012) 127-134.
[21] M.R. Apelian, J.R. Boulton, A.S. Fung, US5284989 (1994), to Mobil Oil.
[22] W.E. Garwood, W. Lee, US4227992 (1980), to Mobil Oil.
[23] W.E. Garwood, W. Lee, US4211640 (1980), to Mobil Oil.
[24] S.J. Miller, GB2106533 (1983), to Chevron.
[25] S.J. Miller, GB2106131 (1983), to Chevron.
[26] S. Han, R.H. Heck, F.T. DiGuiseppi, US5234875 (1993), to Mobil Oil Corporation.
[27] W.H. Verrelst, L.R.M. Martens, WO95/22516 (1995), to Exxon Chemical Patents Inc.
[28] W.H. Verrelst, L.R.M. Martens, US6143942 (2000), to
[29] W.H. Verrelst, L.R.M. Martens, J.P. Verduijn, US6013851 (2006), to
[30] J.A. Martens, J.P. Verduijn, WO95/19945 (1995), to Exxon Chemical Patents Inc.
[31] J.S. Godmarks, G.M.K. Mathys, H.J. Beckers, C.M. Yarbrough, S.H. Brown, Y.-M. Lim, WO2007104385 (2007), to EXXONMOBIL CHEMICAL PATENTS INC.
[32] S.H. Brown, G.M. Mathys, US2007213576 (2007), to EXXONMOBIL CHEMICAL PATENTS INC.
[33] J.A. Martens, W.H. Verrelst, G.M. Mathys, S.H. Brown, P.A. Jacobs, Angewandte Chemie, 117 (2005) 5833-5836.
[34] J.A. Martens, R. Ravishankar, I.E. Mishin, P.A. Jacobs, Angewandte Chemie International Edition, 39 (2000) 4376-4379.
[35] S.A. Tabak, US4254295 (1981), to Mobil Oil.
[36] J.P.G. Pater, P.A. Jacobs, J.A. Martens, Journal of Catalysis, 179 (1998) 477-482.
[37] C.A. Emeis, Journal of Catalysis, 141 (1993) 347-354.
[38] C. Perego, S. Peratello, Catalysis Today, 52 (1999) 133-145.

[39] J. Perez-Ramirez, C.H. Christensen, K. Egeblad, C.H. Christensen, J.C. Groen, Chem. Soc. Rev., 37 (2008) 2530-2542.
[40] D. Verboekend, S. Mitchell, M. Milina, J.C. Groen, J. Perez-Ramirez, J. Phys. Chem. C, 115 (2011) 14193-14203.
[41] D. Verboekend, J. Perez-Ramirez, Catal. Sci. Technol., 1 (2011) 879-890.
[42] R. Chal, C. Gérardin, M. Bulut, S. van Donk, ChemCatChem, 3 (2011) 67-81.
[43] A.N.C. van laak, R.W. Gosselink, S.L. Sagala, J.D. Meeldijk, P.E. de Jongh, K.P. de Jong, Applied Catalysis A: General, 382 (2010) 65-72.
[44] D. Tzoulaki, A. Jentys, J. Perez-Ramirez, K. Egeblad, J.A. Lercher, Catal. Today, (2012) Ahead of Print.
[45] S. Han, US5234875 (1993), to Mobil Oil.
[46] M. Guisnet, P. Magnoux, Applied Catalysis, 54 (1989) 1-27.
[47] G.A. Doka Nassionou, P. Magnoux, M. Guisnet, Journal de Chimie Physique et de Physico-Chimie Biologique, 96 (1999) 303-318.

**FIGURE CAPTION:**

Figure 1. SEM images for commercial MFI samples. a) CBV3020, b) CBV5020, c) CBV8020, d) TZP322, e) TZP302A, f) TZP302H

Figure 2. TEM images for commercial MFI samples. a) CBV3020, b) CBV5020, c) CBV8020, d) TZP322, e) TZP302A, f) TZP302H

Figure 3. $^{27}$Al MAS NMR spectra of the as supplied ZSM-5 samples. a) Zeolyst, b) TRICAT, c) $^{27}$Al MAS NMR measurements of as supplied, calcined (H-) and desilicated (NaOH 0.5 M, 85 ºC, 90 min) –A and OX samples.

Figure 4: TEM images of desilicated MFI: 0.2-TZP322-85-30-OX (a), 0.5-TZP322-85-90-OX (b), 0.8-TZP322-85-90-OX (c), 0.2-TZP322-85-90-A (d), 0.2-CBV5020-85-30-OX (e), and 0.5-CBV5020-85-90-OX (f). Scale bar: 200 nm.

Figure 5: Propene conversion vs. TOS and selectivity within the accumulated C5+ liquid fraction (TOS=0-3 h and TOS=3-6 h) for the un-modified commercial ZSM-5 samples. T=200ºC, P=4.0 MPa, $\tau$=0.17 h, $C_3^=$:$C_3$ = 60:40 (molar).

Figure 6. Correlation of second order kinetic reaction rate constant and Brønsted acid site density for as supplied commercial ZSM-5 samples.

Figure 7: DTG (a) and TPO (b) profiles obtained for spent TZP322 and TZP302H after 6 h TOS.

Catalysts used for oligomerization of propene at T=200ºC, P=4.0 MPa, $\tau$=0.17 h, and with a $C_3^=$:$C_3$ = 60:40 (molar).

Figure 8: Propene conversion Vs. TOS and selectivity within the accumulated C5+ liquid fraction (TOS=0-3 h and TOS=3-6 h) for post-synthesis modified TZP322 based samples. T=200ºC, P=4.0 MPa, $\tau$=0.17 h, $C_3^=$:$C_3$ = 60:40 (molar).

Figure 9: Propene oligomerization. Effect of calcination before NaOH treatment on the catalytic behaviour of TZP322 based samples. T=200ºC, P=40 bar, $\tau$=0.08.

Figure 10: Propene conversion Vs. TOS and selectivity within the accumulated C5+ liquid fraction (TOS=0-3 h and TOS=3-6 h) for post-synthesis modified Zeolyst CBV5020 based samples. T=200ºC, P=4.0 MPa, $\tau$=0.17 h, $C_3^=$:$C_3$ = 60:40 (molar).

Figure 11: Olefin conversion Vs. TOS and selectivity within the accumulated C5+ liquid fraction (TOS=0-3 h and TOS=3-6 h) for as supplied TZP322 sample at two different contact times, 0.08 h (light symbols) and 0.17 h (dark symbols) for propene (triangles) and 1-pentene (circles) oligomerization. T=200ºC, P=40 bar, 40 mol% olefin in the feed.

Figure 12: 1-Pentene conversion Vs. TOS and selectivity within the accumulated C5+ liquid fraction (TOS=0-3 h and TOS=3-6 h) for as supplied (circles) and modified (diamonds) TZP322 samples at two different contact times, 0.08 h (light symbols) and 0.17 h (dark symbols) 1-pentene oligomerization. T=200ºC, P=40 bar, 40 mol% olefin in the feed.

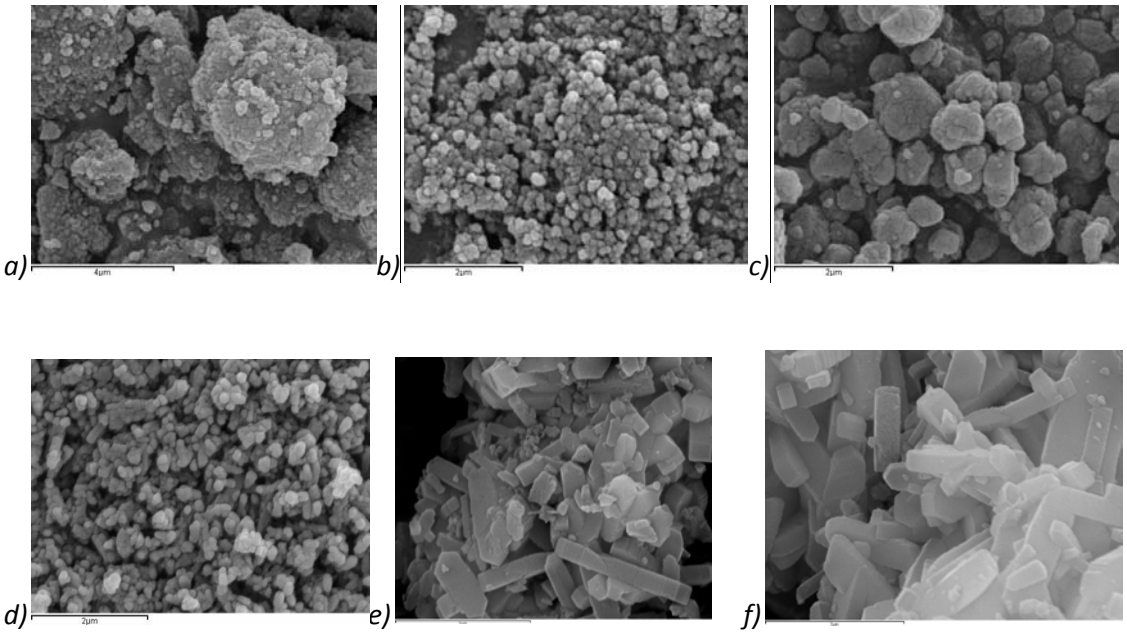


*Figure 1. Representative SEM images for commercial MFI samples. a) CBV3020, b) CBV5020, c) CBV8020, d) TZP322, e) TZP302A, f) TZP302H*

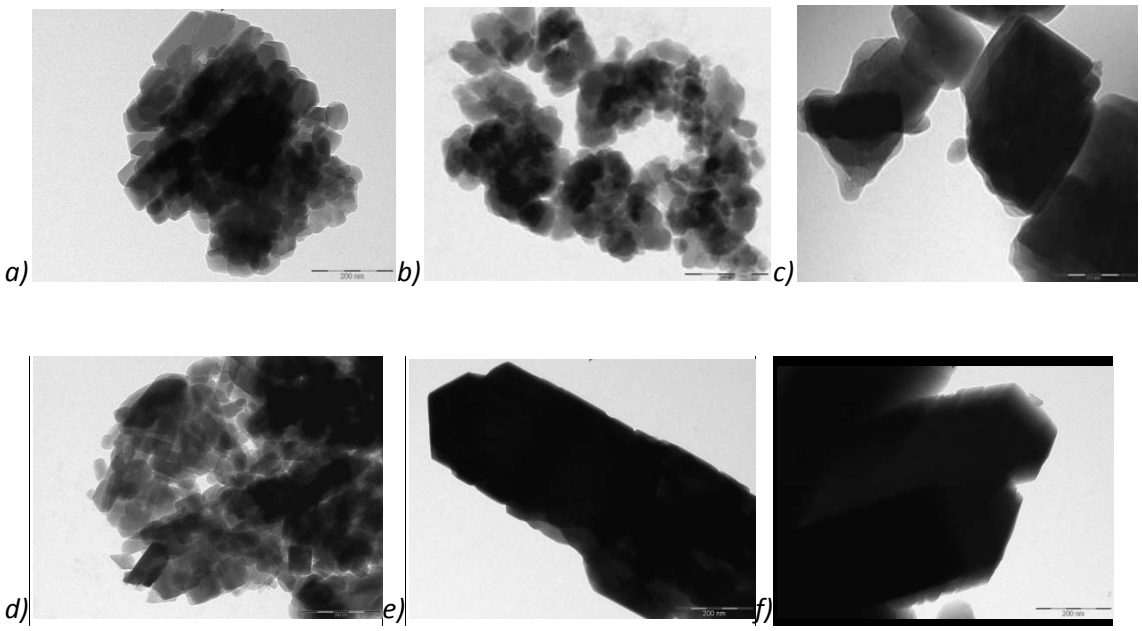


*Figure 2. Representative TEM images for commercial MFI samples. a) CBV3020, b) CBV5020, c) CBV8020, d) TZP322, e) TZP302A, f) TZP302H. Scale bar is 200 nm for all pictures.*

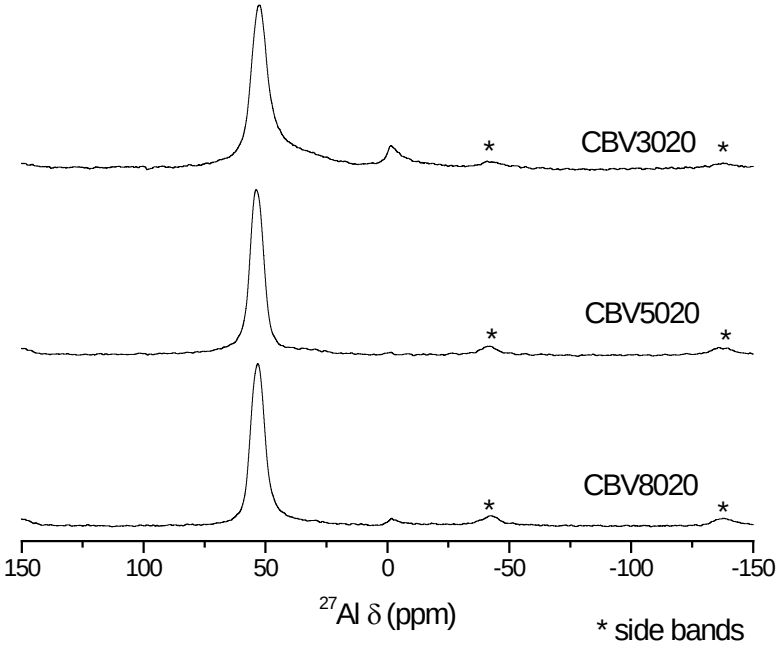
CBV3020
CBV5020
CBV8020
*
150
100
50
0
-50
-100
-150
27Al δ (ppm)
* side bands

a)

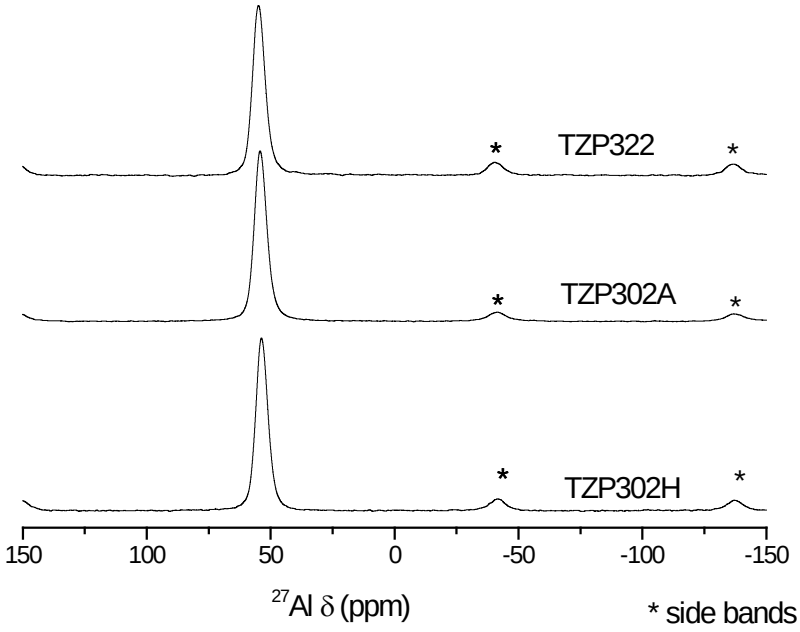
TZP322
TZP302A
TZP302H
*
150
100
50
0
-50
-100
-150
27Al δ (ppm)
* side bands

b)

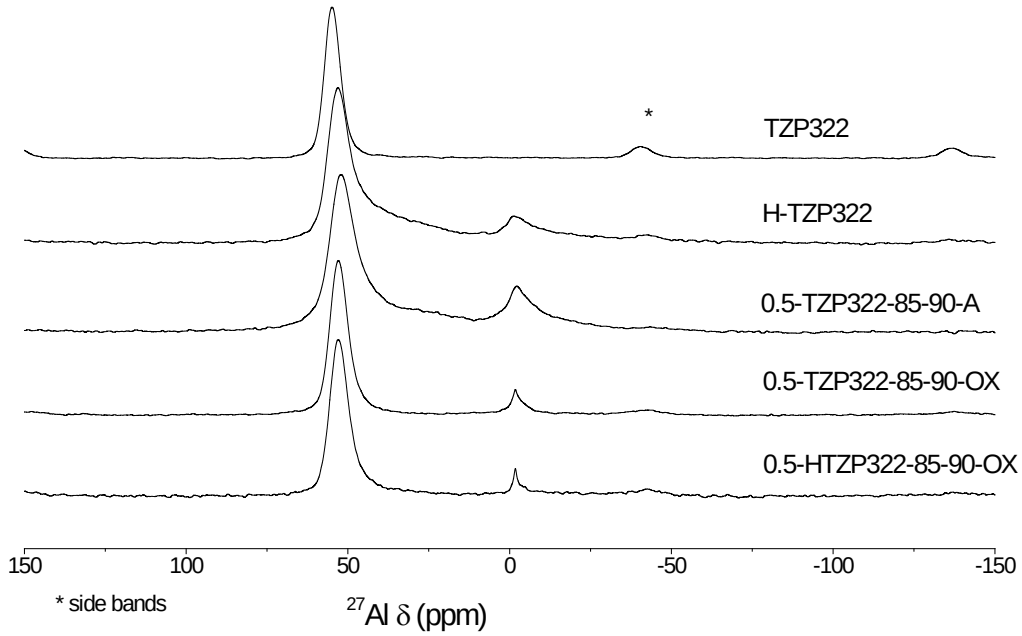


c)

*Figure 3. $^{27}$Al MAS NMR spectra of the as supplied ZSM-5 samples. a) Zeolyst, b) TRICAT*, c) $^{27}$Al MAS NMR measurements of as supplied, calcined (H-) and desilicated (NaOH 0.5 M, 85 ºC, 90 min) –A and OX samples.

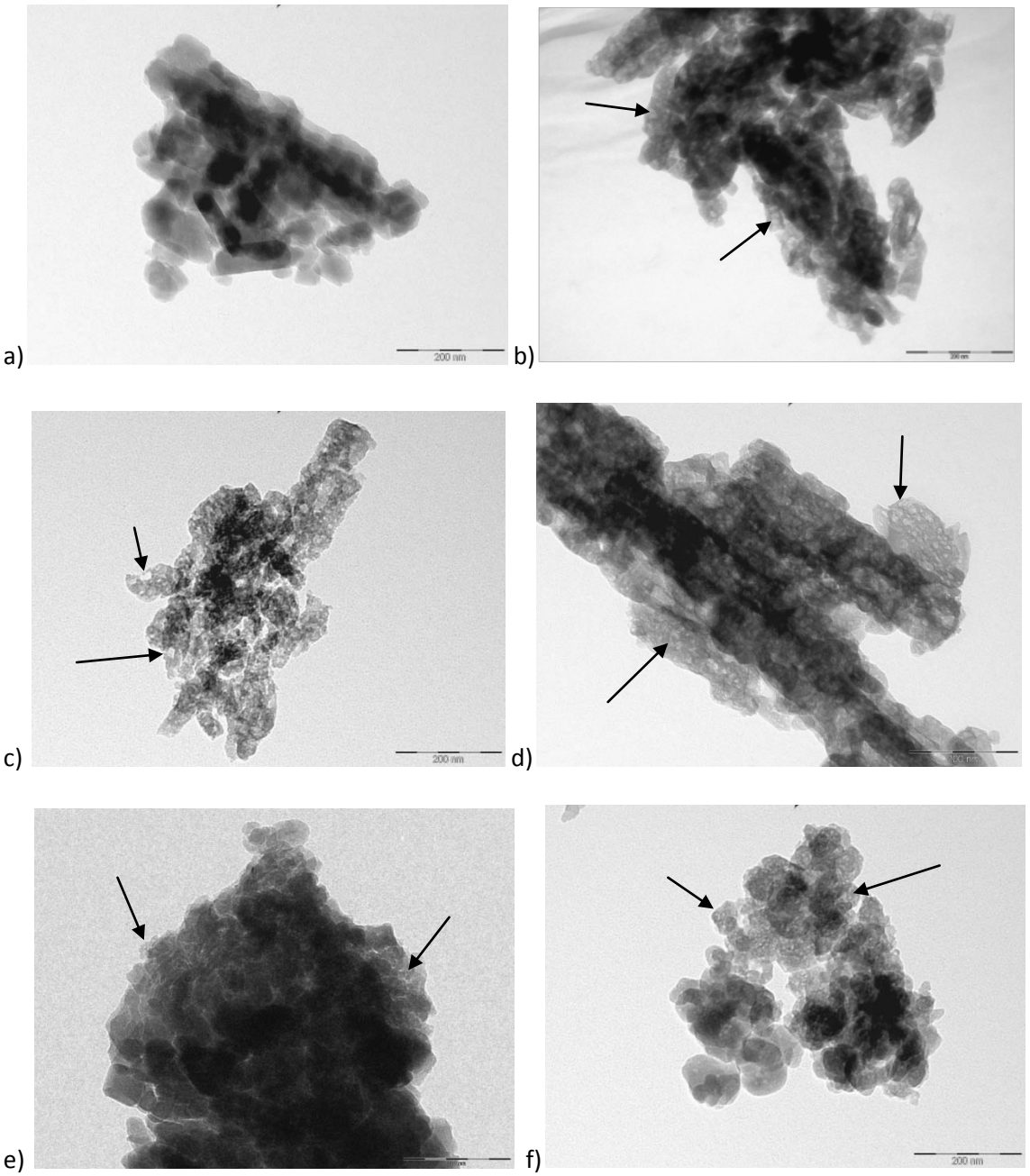


*Figure 4: Representative TEM images of desilicated MFI: 0.2-TZP322-85-30-OX (a), 0.5-TZP322-85-90-OX (b), 0.8-TZP322-85-90-OX (c), 0.2-TZP322-85-90-A (d), 0.2-CBV5020-85-30-OX (e), and 0.5-CBV5020-85-90-OX (f). Scale bar: 200 nm. Arrows indicate the presence of mesopores.*

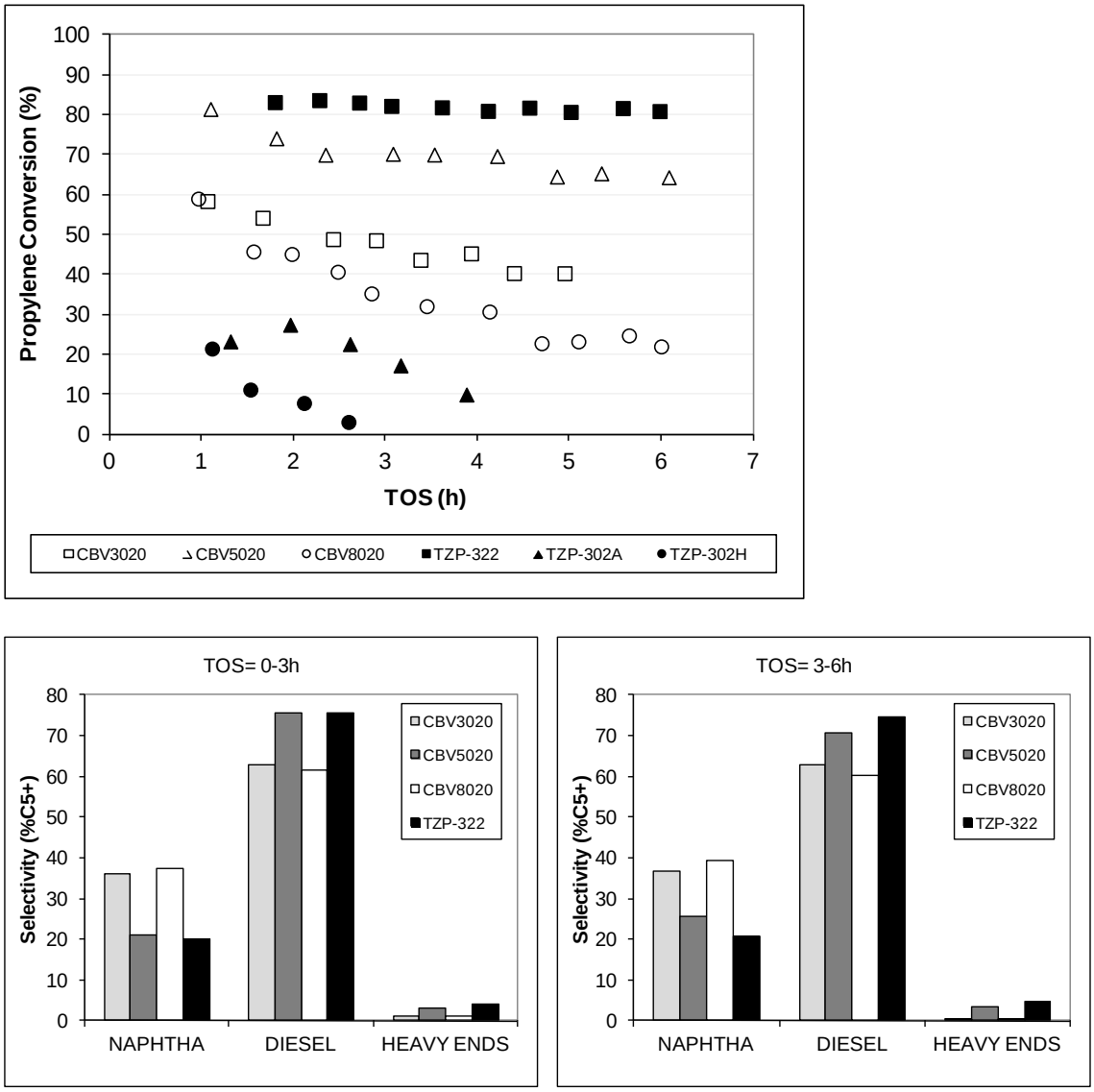


*Figure 5: Propene conversion vs. TOS and selectivity within the accumulated C5+ liquid fraction (TOS=0-3 h and TOS=3-6 h) for the un-modified commercial ZSM-5 samples. T=200ºC, P=4.0 MPa, $\tau$=0.17 h, $C_3^=$:$C_3$ = 60:40 (molar).*

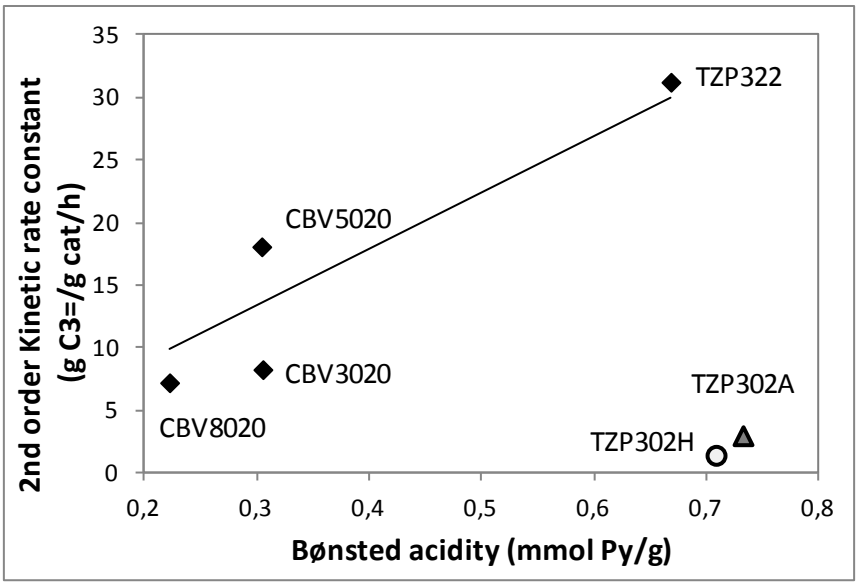


*Figure 6. Correlation of second order kinetic reaction rate constant and Brønsted acid site density for as supplied commercial ZSM-5 samples..*

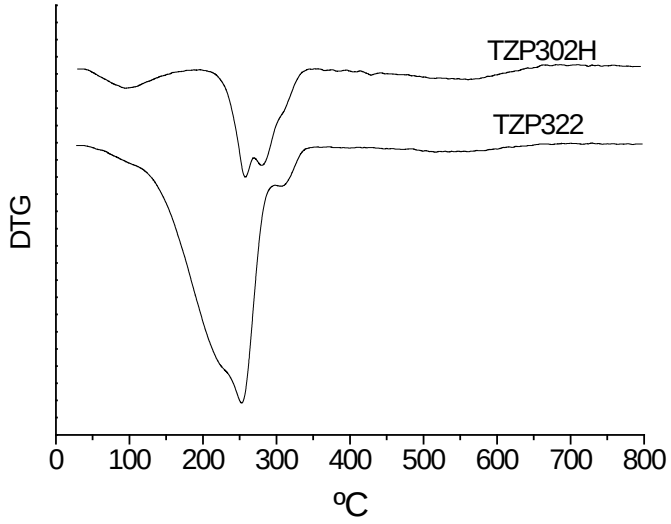


a)

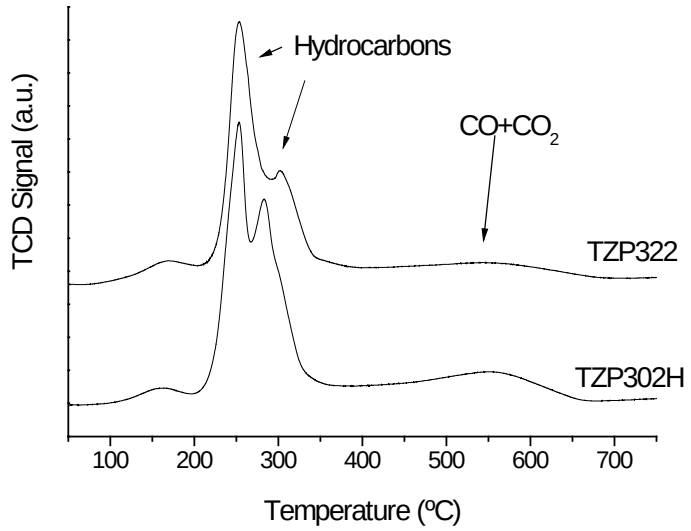


b)

*Figure 7: DTG (a) and TPO (b) profiles obtained for spent TZP322 and TZP302H after 6 h TOS. Catalysts used for oligomerization of propene at T=200ºC, P=4.0 MPa, $\tau$=0.17 h, and with a $C_3^=$:$C_3$ = 60:40 (molar).*

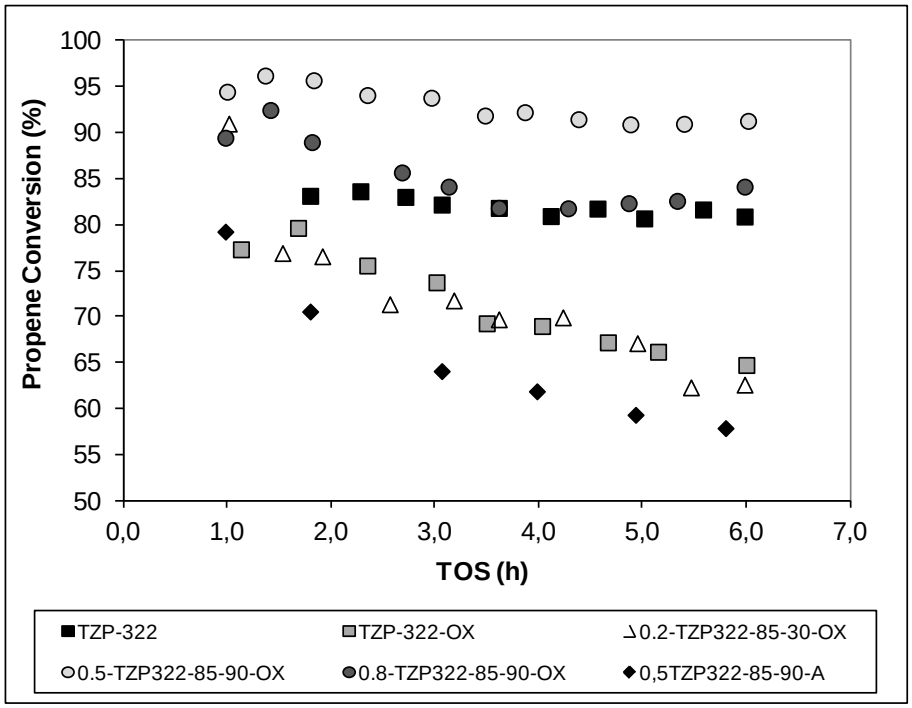


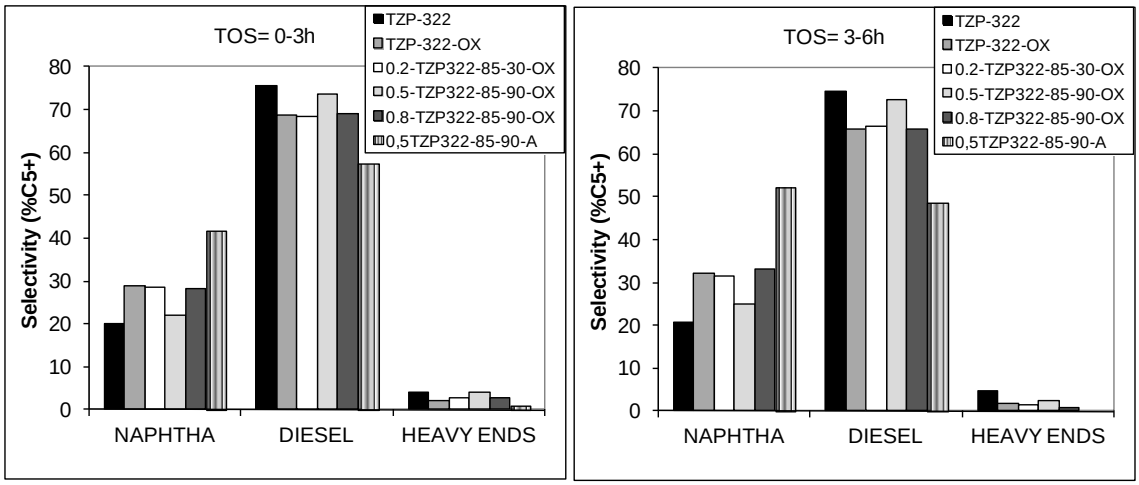


*Figure 8: Propene conversion Vs. TOS and selectivity within the accumulated C5+ liquid fraction (TOS=0-3 h and TOS=3-6 h) for post-synthesis modified TZP322 based samples.*

*T=200ºC, P=4.0 MPa, $\tau$=0.17 h, $C_3^=$:$C_3$ = 60:40 (molar).*

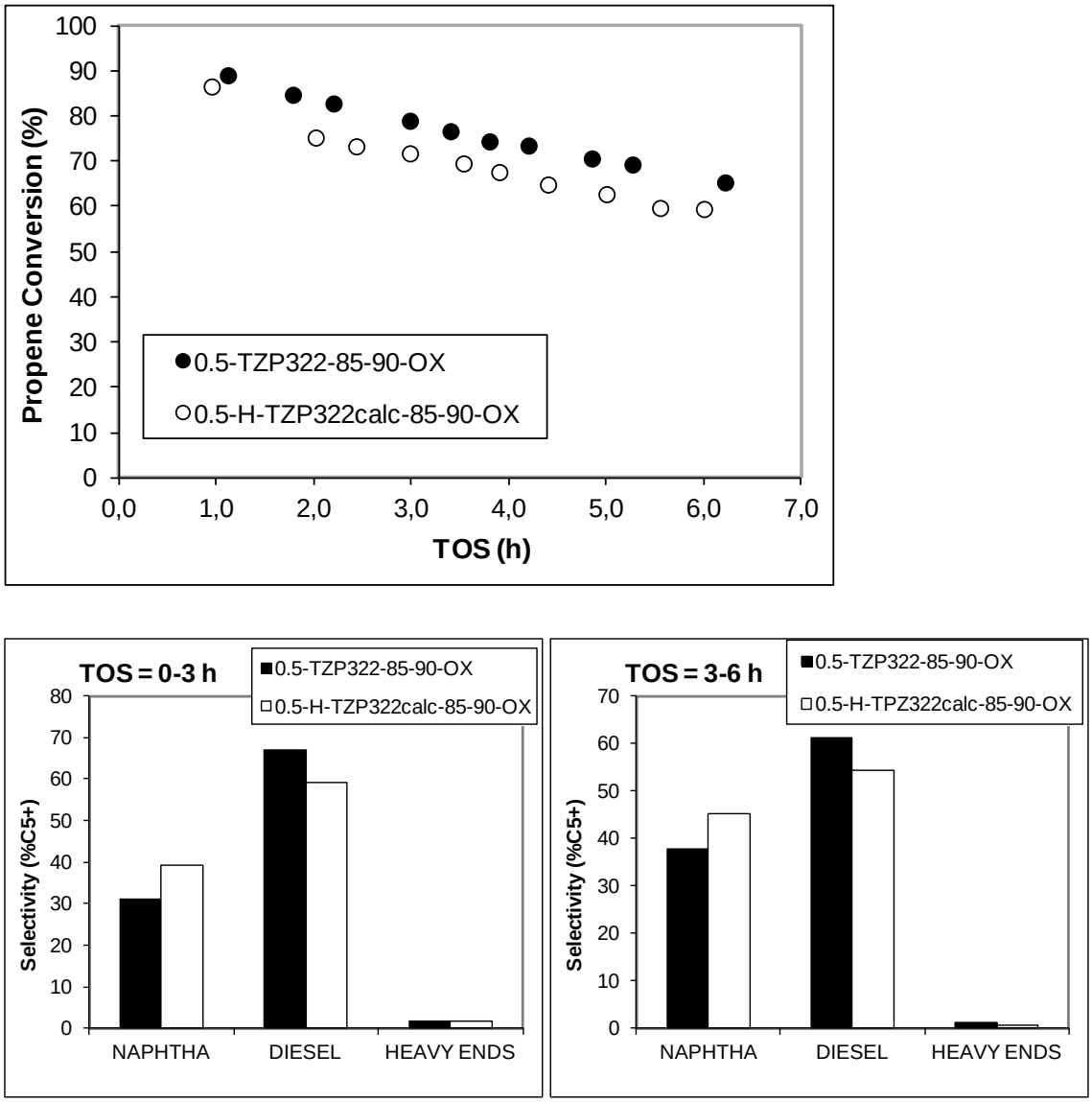


*Figure 9: Propene oligomerization. Effect of calcination before NaOH treatment on the catalytic behaviour of TZP322 based samples. T=200ºC, P=40 bar, $\tau$=0.08.*

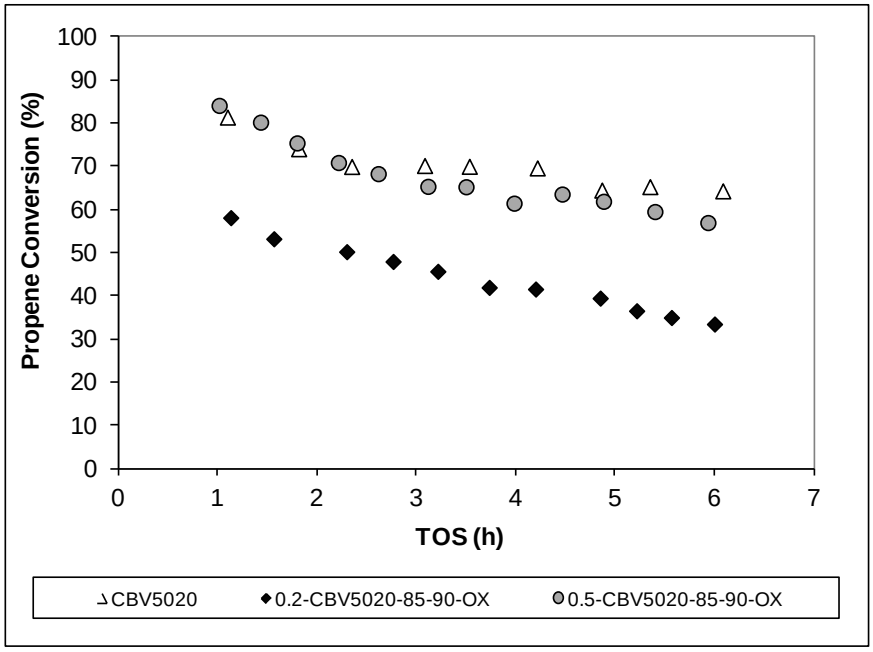


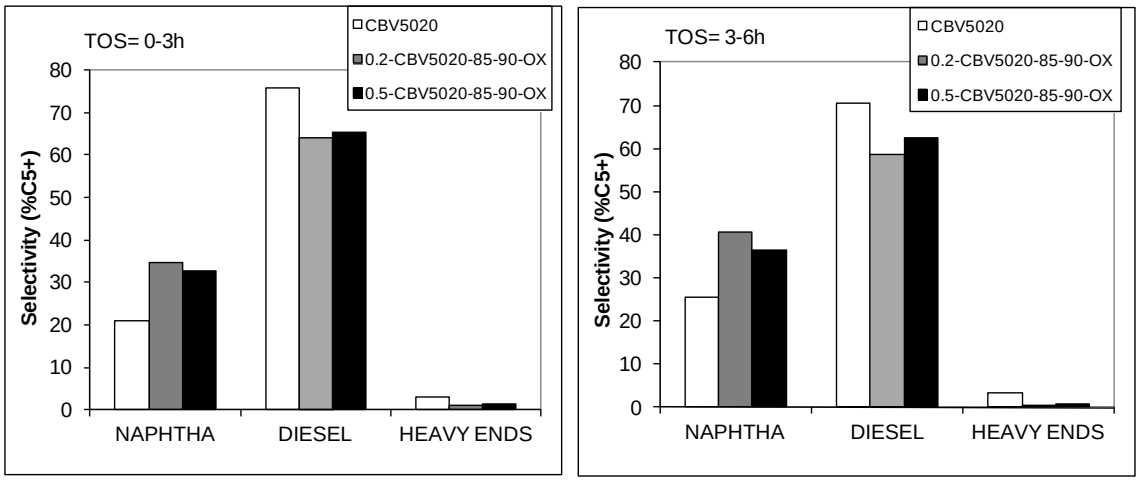


*Figure 10: Propene conversion Vs. TOS and selectivity within the accumulated C5+ liquid fraction (TOS=0-3 h and TOS=3-6 h) for post-synthesis modified Zeolyst CBV5020 based samples. T=200ºC, P=4.0 MPa, $\tau$=0.17 h, $C_3^=$:$C_3$ = 60:40 (molar).*

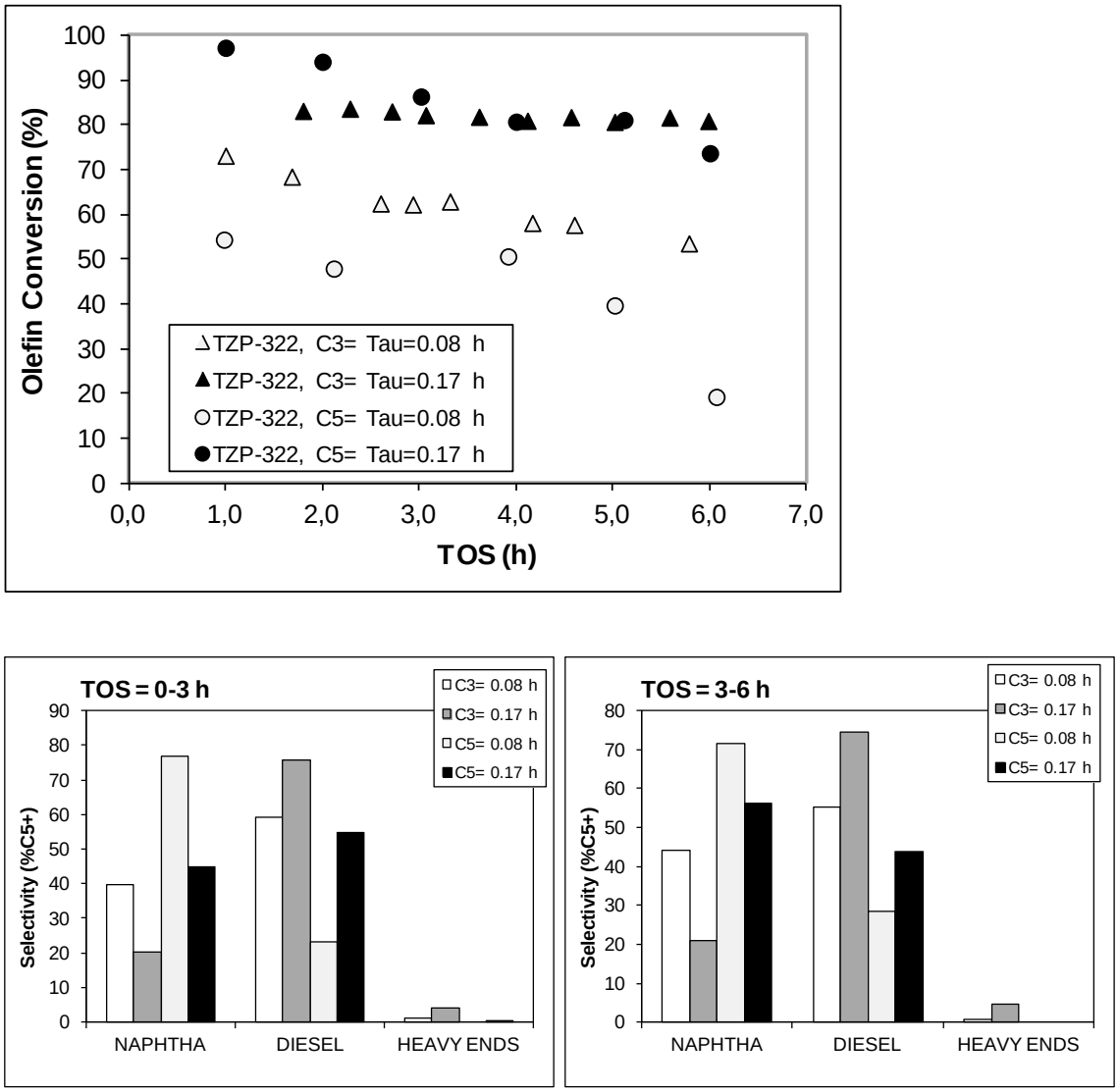


*Figure 11: Olefin conversion Vs. TOS and selectivity within the accumulated C5+ liquid fraction (TOS=0-3 h and TOS=3-6 h) for as supplied TZP322 at two different contact times, 0.08 h (light symbols) and 0.17 h (dark symbols) for propene (triangles) and 1-pentene (circles) oligomerization. T=200ºC, P=4.0 MPa, 40 mol% olefin in the feed.*

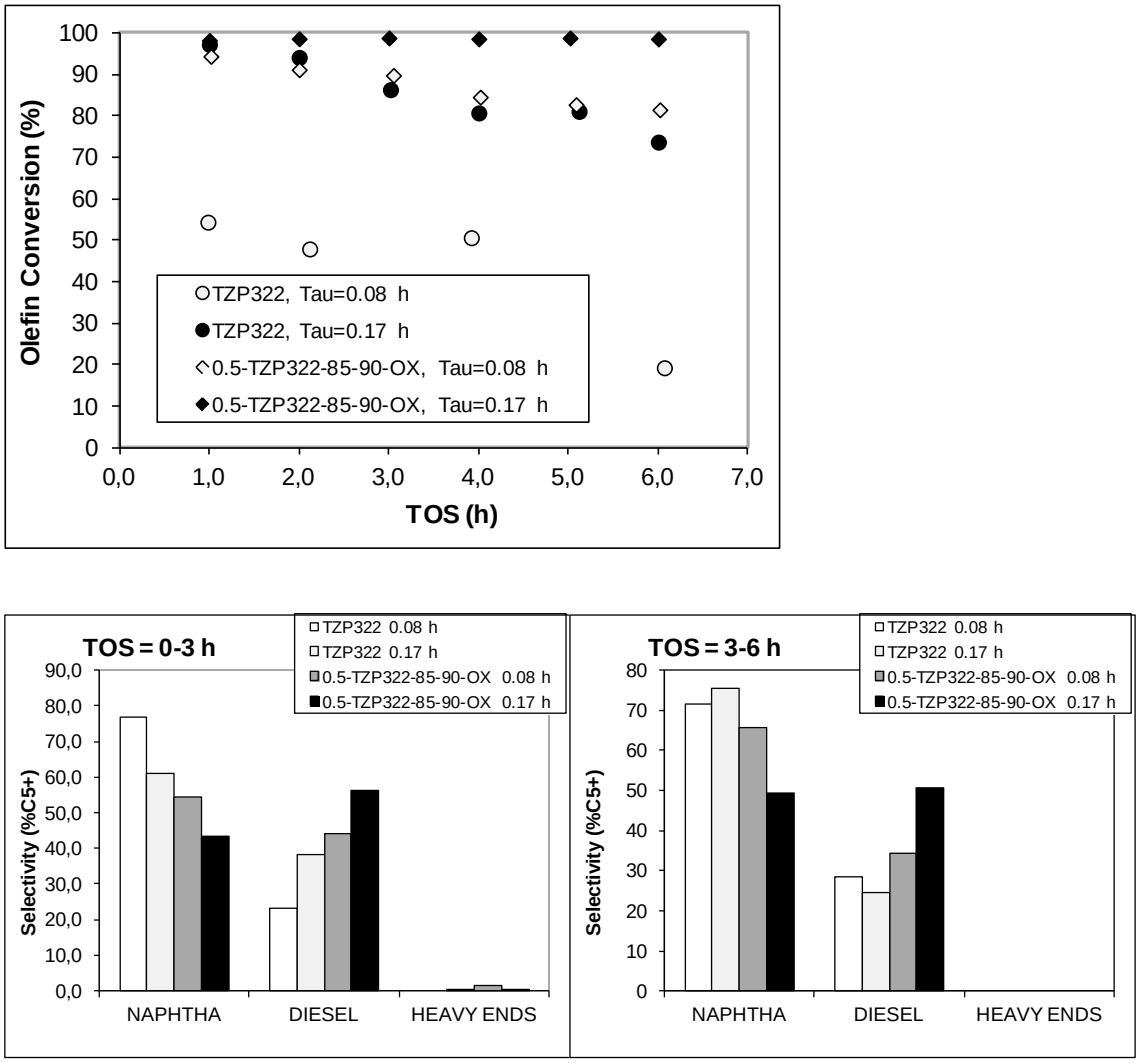


*Figure 12: 1-Pentene conversion Vs. TOS and selectivity within the accumulated C5+ liquid fraction (TOS=0-3 h and TOS=3-6 h) for as supplied (circles) and modified (diamonds) TZP322 samples at two different contact times, 0.08 h (light symbols) and 0.17 h (dark symbols) 1-pentene oligomerization. T=200ºC, P=4.0 MPa, 40 mol% olefin in the feed.*

*Table 1. Physico-chemical properties of as supplied commercial MFI samples.*

| Sample | Average crystal size (nm) | $Si/Al)_{Supplier}$ | $Si/Al)_{ICP}$ | BET ($m^2/g$) | $V_{micropore}$ ($cm^3/g$) | $V_{mesopore}$ ($cm^3/g$) |
|---|---|---|---|---|---|---|
| CBV3020 | 200 | 15 | 15 | 397 | 0.160 | 0.110 |
| CBV5020 | 163 | 25 | 20 | 375 | 0.154 | 0.085 |
| CBV8020 | 580 | 40 | 31 | 389 | 0.168 | 0.072 |
| TZP-322 | 173 | 15 | 11 | 391 | 0.168 | 0.112 |
| TZP-302A | 912 | 15 | 10 | 364 | 0.171 | 0.058 |
| TZP-302H | 1805 | 15 | 10 | 373 | 0.173 | 0.046 |

*Table 2. Acidity of as supplied commercial MFI samples as measured by FT-IR combined with pyridine adsorption and desorption at increasing temperatures.*

| Catalyst | Acidity (mmol Pyridine/g) | | | | | |
|---|---|---|---|---|---|---|
| | Brønsted | | | Lewis | | |
| | T=150ºC | T=250ºC | T=350ºC | T=150ºC | T=250ºC | T=350ºC |
| CBV3020 | 0.305 | 0.232 | 0.191 | 0.062 | 0.050 | 0.047 |
| CBV5020 | 0.304 | 0.276 | 0.212 | 0.022 | 0.010 | 0.015 |
| CBV8020 | 0.222 | 0.213 | 0.173 | 0.022 | 0.015 | 0.013 |
| TZP-322 | 0.668 | 0.629 | 0.398 | 0.015 | 0.021 | 0.019 |
| TZP-302A | 0.733 | 0.563 | 0.368 | 0.019 | 0.012 | 0.006 |
| TZP-302H | 0.709 | 0.516 | 0.455 | 0.015 | 0.008 | 0.005 |

*Table 3. Physico-chemical properties of desilicated MFI samples.*

| Sample | Si/Al (ICP) | Si/Al (XPS) | BET ($m^2/g$) | $V_{micropore}$ ($cm^3/g$) | $V_{mesopore}$ ($cm^3/g$) | Yield (wt%) |
|---|---|---|---|---|---|---|
| TZP322 | 11 | 21 | 391 | 0.168 | 0.112 | --- |
| TZP322-OX | 14 | 35 | 382 | 0.166 | 0.222 | --- |
| 0.2-TZP322-65-30-OX | 14 | n.d.* | 390 | 0.165 | 0.138 | 86 |
| 0.2-TZP322-85-30-OX | 16 | n.d. | 396 | 0.163 | 0.144 | 79 |
| 0.5-TZP322-85-90-OX | 19 | 31 | 483 | 0.158 | 0.299 | 65 |
| 0.8-TZP322-85-90-OX | 34 | n.d. | 547 | 0.146 | 0.500 | 34 |
| 0.5-TZP322-85-90-A | 7 | 7 | 385 | 0.105 | 0.192 | 60 |
| HTZP322 | 11 | n.d. | 380 | 0.163 | 0.113 | --- |
| 0.5-HTZP322-85-90-OX | 29 | n.d. | 530 | 0.162 | 0.362 | 65 |
| CBV5020 | 24 | n.d. | 375 | 0.154 | 0.085 | --- |
| 0.2-CBV5020-85-30-OX | 19 | n.d. | 406 | 0.147 | 0.245 | 76 |
| 0.2-CBV5020-85-90-OX | 28 | n.d. | 431 | 0.161 | 0.267 | 66 |
| 0.5-CBV5020-85-90-OX | 47 | n.d. | 513 | 0.142 | 0.856 | 43 |

** n.d.: not determined.*

*Table 4. Acidity of post-synthesis modified MFI based samples as measured by FT-IR combined with pyridine adsorption and desorption at increasing temperatures.*

| Catalyst | Acidity (mmol Pyridine/g) | | | | | |
|---|---|---|---|---|---|---|
| | Brønsted | | | Lewis | | |
| | T=150ºC | T=250ºC | T=350ºC | T=150ºC | T=250ºC | T=350ºC |
| TZP-322 | 0.668 | 0.629 | 0.398 | 0.015 | 0.021 | 0.019 |
| TZP-322-OX | 0.453 | 0.428 | 0.299 | 0.033 | 0.026 | 0.031 |
| 0.2-TZP322-85-30-OX | 0.353 | 0.332 | 0.243 | 0.037 | 0.026 | 0.037 |
| 0.5-TZP322-85-90-OX | 0.253 | 0.269 | 0.175 | 0.037 | 0.039 | 0.041 |
| 0.8-TZP322-85-90-OX | 0.175 | 0.158 | 0.102 | 0.039 | 0.033 | 0.031 |
| 0.5-TZP322-85-90-A | 0.292 | 0.232 | 0.220 | 0.110 | 0.089 | 0.87 |
| H-TZP-322 | 0.371 | 0.282 | 0.213 | 0.055 | 0.056 | 0.050 |
| 0.5-H-TZP322-85-90-OX | 0.164 | 0.170 | 0.109 | 0.032 | 0.035 | 0.030 |
| CBV5020 | 0.304 | 0.276 | 0.212 | 0.022 | 0.010 | 0.015 |
| 0.2-CBV5020-85-30-OX | 0.225 | 0.192 | 0.206 | 0.018 | 0.011 | 0.018 |
| 0.2-CBV5020-85-90-OX | 0.125 | 0.104 | 0.65 | 0.018 | 0.015 | 0.015 |
| 0.5-CBV5020-85-90-OX | 0.135 | 0.109 | 0.78 | 0.025 | 0.022 | 0.025 |